RNA helicase, DDX27 regulates proliferation and myogenic commitment of muscle stem cells

Short Title: Translational Regulation of Myogenesis by DDX27

Alexis H Bennett[1], Marie-Francoise O'Donohue[2], Stacey R. Gundry[3], Aye T. Chan[4], Jeffery Widrick[3], Isabelle Draper[5,] Anirban Chakraborty[2], Yi Zhou[4], Leonard I. Zon[4,6], Pierre-Emmanuel Gleizes[2], Alan H. Beggs[3], Vandana A Gupta[1,3]*

1. Division of Genetics, Brigham and Women's Hospital, Harvard Medical School, Boston MA 02115, USA

2. Laboratoire de Biologie Moléculaire Eucaryote, Centre de Biologie Intégrative (CBI), Université de Toulouse, UPS, CNRS, France

3. Division of Genetics and Genomics, The Manton Center for Orphan Disease Research, Boston Children's Hospital, Harvard Medical School, Boston, MA 02115, USA.

4.Stem Cell Program and Pediatric Hematology/Oncology, Boston Children's Hospital and Dana Farber Cancer Institute, Harvard Stem Cell Institute, Harvard Medical School, Boston, MA 02115, USA.

5. Molecular Cardiology Research Institute, Tufts Medical Center, Boston, MA 02111, USA

6. Howard Hughes Medical Institute.

*Corresponding Author

Vandana A Gupta
Division of Genetics,
Department of Medicine,
Brigham and Women's Hospital,
Harvard Medical School,
Boston, MA 02115.
Email: vgupta@research.bwh.harvard.edu

ABSTRACT

Developmental processes depend on the combined efforts of epigenetic, transcriptional and post-transcriptional processes that lead to the production of specific proteins that are important determinants of cellular identity and developmental processes. Ribosomes are a central component of the protein biosynthesis machinery in cells; however, their regulatory roles in the translational control of gene expression in an organ specific context during development remain to be defined. In a genetic screen to identify critical regulators of myogenesis, we identified a DEAD-Box RNA helicase, DDX27, that is required for the proliferation and myogenic commitment of skeletal muscle stem cells. DDX27 deficient skeletal muscle exhibits hypotrophy and impaired regeneration potential. We demonstrate that DDX27 regulates ribosomal RNA (rRNA) maturation, and thereby the ribosome biogenesis and the translation of specific transcripts that are required to maintain pluripotency and myogenic differentiation of satellite cells. These findings provide insight into the translational regulation of gene expression in myogenesis and suggest novel functions for ribosomes in regulating gene expression during skeletal muscle development.

AUTHOR SUMMARY

Inherited skeletal muscle diseases are the most common form of genetic disorders with primary abnormalities in the structure and function of skeletal muscle resulting in the impaired locomotion in affected patients. A major hindrance to the development of effective therapies is a lack of understanding of biological processes that promote skeletal muscle growth. By performing a forward genetic screen in zebrafish we have identified mutation in a RNA helicase that leads to perturbations of ribosomal biogenesis pathway and impairs skeletal muscle growth and regeneration. Therefore, our studies have identified novel ribosome-based disease processes that may be therapeutic modulated to restore muscle function in skeletal muscle diseases.

KEYWORDS

Skeletal muscle, muscle stem cells, satellite cells, differentiation, rRNA processing, ribosome, translational regulation, gene expression.

INTRODUCTION

Ribosome biogenesis is fundamental to all life forms and is the primary determinant of translational capacity of the cell. Ribosome biogenesis is a complex process that involves transcription, modification and processing of ribosomal RNA, production of ribosomal proteins and auxiliary factors and coordinated assembly of ribonucleoprotein complexes to produce functional ribosomes [1]. While previously considered a “house keeping” constitutive process, recent studies have shown that ribosome biogenesis is

regulated differently between cells and can be modulated in a cell type-specific manner [2]. These differences are required to generate ribosomes of different heterogeneities and functionalities that contribute to the translational control of gene regulation by selecting mRNA subsets to be translated under specific growth conditions potentially by identifying specific recognition elements in the mRNA [3-5]. Protein synthesis is the end stage of the gene regulation hierarchy and despite the identification of translational regulators of specific genes, a systematic identification of translational regulatory processes critical for tissue specific control of gene expression is still lacking. Moreover, upstream regulatory factors/processes that regulate ribosome heterogeneity in a cellular and organ-specific context in vertebrates still remains to be identified.

Skeletal muscle is a contractile, post-mitotic tissue that accounts for 30-50% of body mass. Skeletal muscle growth and repair is a highly coordinated process that is dependent on the proliferative expansion and differentiation of muscle stem cells that originate from the muscle progenitor cells at the end of embryogenesis [6-8]. Activated muscle stem cells through symmetric/ asymmetric divisions give rise to daughter cells that maintain the muscle stem cell population (satellite cells) and committed myogenic precursor cells that fuse to form the differentiated skeletal muscle [6, 9, 10]. Defects in processes regulating muscle stem cells, myoblast fusion and differentiation therefore, constitute pathological pathways regulating the muscle growth and regeneration during development and diseases [11-13]. Although epigenetic and transcriptional controls of myogenesis have been studied extensively, the importance of translational regulation of these processes in skeletal muscle development is less defined. Transcriptional and translational analysis of myoblasts has shown that differential mRNA translation controls protein expression of specific subset of genes during myogenesis. Recent studies have

revealed ribosomal changes during skeletal muscle growth and atrophy. An increase in ribosome biogenesis is often observed during skeletal muscle hypertrophy [14, 15]. Ribosomal perturbations on the other hand are associated with skeletal muscle growth and diseases [16-19]. Deletion of ribosomal protein genes *S6k1* and *Rps6* in mice results in smaller myofibers and reduced muscle function. In several muscular dystrophy models and atrophied muscles, a reduction in ribosome number and/or activity is observed [18, 20, 21]. Inspite of dynamic changes observed in ribosomes during different growth conditions, our understanding of the mechanism(s) that regulate ribosomal biogenesis in skeletal muscle and eventually control the translational landscape during muscle growth is still poor.

In a forward genetic screen to identify critical regulators of myogenesis *in vivo*, we recently identified a RNA helicase gene, *ddx27*, that controls skeletal muscle growth and regeneration in zebrafish [22, 23]. We further show that Ddx27 is required for rRNA maturation and ribosome biogenesis. Strikingly, *Ddx27* deficient myoblasts exhibit impaired translation of mRNA transcripts that control RNA metabolism and proliferation as well as differentiation of muscle stem cells. These studies highlight the specific role of upstream ribosome biogenesis processes in regulating tissue specific gene expression during myogenesis.

RESULTS

Identification of novel regulators of myogenesis *in vivo*

Zebrafish and human exhibit similar skeletal muscle structure and the molecular regulatory hierarchy of skeletal muscle development is conserved between zebrafish and mammals [9, 24]. Therefore, to identify regulators of skeletal muscle development and disease *in vivo*, we performed an ENU mutagenesis screen in zebrafish [22].

Analysis of skeletal muscle of 4-5 dpf (days post fertilization) larvae of one mutant identified in the screen, *Osoi* (Japanese for "slow"), displayed highly reduced birefringence in polarized light microscopy in comparison to the control, indicative of skeletal muscle defects (Fig 1A). Positional mapping and sequencing of this mutation identified a 20 bp deletion in exon 18 of the *ddx27* gene (DEAD-box containing RNA helicase 27) (Fig 1B, S1A and B). qRT-PCR analysis showed significantly lower levels of *ddx27* transcripts reflecting probable nonsense-mediated decay (S1C Fig). Overexpression of human *DDX27* resulted in a rescue of skeletal muscle defects in mutant embryos, demonstrating functional evolutionary conservation and confirming that mutation in *ddx27* are causal for the *osoi* phenotype (S1D Fig). Evaluation of a large number of mutant embryos showed that homozygotes die by 6-7 dpf. qRT-PCR analysis of mouse *Ddx27* mRNA in different tissues demonstrated *Ddx27* expression in several tissue types (*S*1E Fig).

To define the functional requirement of *DDX27* in different organs, tissue-specific RNAi-mediated knockdown of *Rs1*, the fly ortholog of human *DDX27,* was carried out in *Drosophila* (using the Gal4/UAS bipartite system) [25]. Downregulation of *Rs1* in the entire organism (using the *Act5C-GAL4* driver) leads to lethality of the developing flies during late larval/pupae stage. The lethality phenotype is recapitulated when *Rs1* knockdown is targeted to skeletal muscles (using the *held out wing* '*how'-GAL4* driver), or to the heart (using the *TinC-GAL4* driver). Of note, targeting Rs1 knockdown in other tissues, i.e. the brain or gastrointestinal tract, was well-tolerated and did not result in gross phenotype in emerging adults (S2 Fig).

To identify DDX27 expression domains in skeletal muscle, immunofluorescence was performed in human skeletal muscle. Examination of skeletal muscle by

immunofluorescence showed DDX27 expression to be restricted to PAX7 expressing nuclei suggesting that DDX27 is expressed in quiescent satellite cells during normal growth (Fig 1C). Cardiotoxin injury of skeletal muscle results in activation and proliferation of muscle satellite cells. To investigate the expression of DDX27 in activated satellite cells, we induced skeletal muscle injury and regeneration by injecting cardiotoxin in the tibialis anterior (TA) muscle and analyzed *Ddx27* expression during the course of muscle regeneration. qRT-PCR revealed a significant upregulation of *Ddx27* in regenerating skeletal muscles 7 days post injury (Fig 1D). These results show that DDX27 is expressed in both quiescent as well as activated satellite cells in skeletal muscle. We next investigated the sub-nuclear expression of DDX27 in human myoblasts. Immunofluorescence revealed that DDX27 co-localized with UBF (fibrillar component) and Fibrillarin (dense fibrillary component) in nucleoli of human myoblasts (Fig 1E). This sub-nucleolar organization of DDX27 suggests a functional requirement of DDX27 in rDNA transcription and/or pre-rRNA processing steps in skeletal muscles.

Precocious skeletal muscle differentiation in Ddx27 deficiency

To investigate the role of RNA helicase Ddx27 in skeletal muscle homeostasis, we analyzed the structure and function of mutant zebrafish larvae. Homozygous *ddx27* mutant fish (5 dpf) showed reduced fiber diameter (Fig 2A-B arrow, inset) and central nuclei as observed in several muscle diseases (Fig 2A-B, arrowhead) [26]. Electron microscopy of longitudinal sections of *ddx27* mutant myofibers also showed disorganized myofibrillar structures in *ddx27* mutant fish (Fig 2C-E, arrow). The mutant myofibers displayed smaller Z-lines and disorganized actin-myosin assemblies in comparison to controls suggesting differentiation defects of these muscles.

Immunofluorescence of cultured myofibers from control and mutant zebrafish further showed a reduction and disorganization of skeletal muscle differentiation markers (Actn2/3 and Ryr1) validating our earlier observation that absence of Ddx27 results in a defective differentiation of skeletal muscles (S3A Fig). The centralized mutant nuclei were round in shape with highly enlarged nucleoli in comparison to controls (Fig 2E, arrowhead). Cross-sections of muscles showed a reduction in myofiber diameter (52 ± 14%) in *ddx27* mutant fish in comparison to controls (Fig 2F-H). Skeletal muscles of mutant fish also displayed whorled membrane structures associated with nuclei (Fig 3F, arrow). These whorled membrane structures are often observed in skeletal muscle of congenital myopathy patients, however their origin and biological significance remains unknown. The birefringence in mutant zebrafish was significantly reduced throughout the development (1-5 dpf) indicative of a differentiation defect rather than muscle degeneration seen in zebrafish models of muscular dystrophies [22, 27]. *Ddx27* knockout murine myoblasts also failed to differentiate that suggests the functions of DDX27 in growth and differentiation of skeletal muscle are conserved in vertebrates (S3B-D Fig).

To identify the molecular events leading to differentiation defects in *ddx27* mutant zebrafish qRT-PCR was performed during embryonic (2 dpf) and larval (4 dpf) stages. qRT-PCR revealed no significant changes in muscle stem cell markers, *pax3* and *pax7* expression during the embryonic stage (Fig 2I). However, significant down regulation of *pax7* mRNA was observed during the larval stage in *ddx27* mutant zebrafish. Concurrently, with a downregulation of muscle stem cells markers (*pax3*, *pax7*), we also observed a high expression of *myoD*, *myf5* and *desmin* in mutant muscles (Fig 2I). Previous studies have shown Pax7 expression in satellite cells is associated with down-

regulation of MyoD expression and inhibition of myogenic commitment indicating that Pax7 inhibits early events in molecular cascade leading to muscle differentiation [28-30]. Therefore, low levels of *pax7* and high level of *myoD* in *ddx27* mutant muscles are likely to produce a premature activation of the myogenic program. However, this precocious activation of the myogenic program appears to be unable to progress to a proper differentiated state, as documented by low levels of late differentiation markers *myog* and *mylz* leading to disorganized sarcomeres and skeletal muscle hypotrophy in the mutant fish. Taken together, these data show that through regulation of early myogenic program, DDX27 controls the myogenic commitment of muscle stem cells and subsequent differentiation of committed myogenic population.

Reduced contractile strength in *ddx27* deficient skeletal muscles

ddx27 zebrafish larvae exhibit significantly slower swimming than wild-type controls at 5 dpf (90.53 $\pm$ 28.69 mm/10 min for *ddx27* vs.1682.92 $\pm$ 213.77 mm/10 min for controls). To quantify the functional deficits in skeletal muscles of homozygous *ddx27* mutant larvae (5 dpf), peak twitch and tetanic forces of individual zebrafish skeletal muscle preparations were measured following electrical stimulation. Substantially depressed twitch and tetanic forces as well as the slower rise and fall of tension were observed in *ddx27* mutants (Fig 3A). Absolute tetanic force was significantly less for *ddx27* larvae compared to controls (mean ± SD: 0.28 ± 0.18 vs. 1.43 ± 0.27 mN; $p < 0.0001$) (Fig 3B). These force deficits in *ddx27* persisted in the force measurements normalized for cross-sectional areas (Fig 3C: 11 ± 8 vs. 48 ± 6 kPa; $p < 0.0001$), suggesting that the depressed tetanic force of the *ddx27* mutant preparations is primarily due to intrinsic skeletal muscle deficits. Mutant *ddx27* preparations also showed significant reductions

in mean absolute twitch force (Fig 3D: 0.16 ± 0.12 vs. 1.11 ± 0.23 mN; $p < 0.0001$) and twitch force normalized to the CSA of individual larvae (Fig 3E: 7 ± 5 vs. 37 ± 4 kPa; $p < 0.0001$). Interestingly, twitch force was depressed to a relatively greater extent than tetanic force as revealed by the significantly reduced twitch to tetanic force ratios of the *ddx27* preparations (Fig 3F: 0.57 ± 0.15 vs. 0.78 ± 0.06 kPa; $p = 0.0006$). In addition to these differences in force magnitude, the kinetics of force development and relaxation were also affected in mutant skeletal muscles. The *ddx27* larvae displayed a significantly slower rise in the maximal rate of twitch tension development, +dP/dt (Fig 3G: 1.06 ± 0.71 vs. 8.00 ± 1.30 kPa/ms; $p < 0.0001$), and a significantly slower maximal rate of twitch tension relaxation, -dP/dt (Fig. 3H: -0.47 ± 0.24 vs. -2.55 ± 0.35 kPa/ms; $p < 0.0001$). This disproportionate reduction in twitch vs. tetanic force and the slowing of twitch kinetics indicate a reduction in the quality of the contractile performance of the *ddx27* larvae that are consistent with reduced motility of mutant muscles.

Reduced muscle stem cells proliferation and impaired regeneration in Ddx27 deficiency

As the expression of muscle stem cell marker, *pax7* was reduced during the larval (4 dpf) stage of zebrafish growth (Fig 2I), we next investigated if this decreased expression was a consequence of a defect in muscle stem cell proliferation or apoptosis. Quantification of Pax7 nuclei by whole mount immunofluorescence showed a significant reduction in Pax7 expressing nuclei (40 ± 8.2%) in mutant skeletal muscle compared with control fish (4 dpf) (Fig 4A). To evaluate the proliferative potential of *Ddx27* deficient muscle satellite cells, we performed 5-ethynyl-2'-deoxyuridine (EdU) incorporation assay that revealed a significant reduction in EdU positive cells in *ddx27*

skeletal muscles, indicating a proliferation defect (Fig 4B). Whole mount TUNEL staining of zebrafish skeletal muscle did not reveal any significant changes in apoptotic nuclei in mutant muscles compared to controls (S4 Fig).

A stem cell niche equivalent to mammalian satellite cell system exists in zebrafish that involves migration and asymmetric division and/or proliferation of muscle stem cells to repair muscle upon injury during larval stages [8, 31]. Therefore to evaluate the role of Ddx27 in skeletal muscle repair during muscle regeneration, cardiotoxin was injected into the epiaxial myotome of somites of larval fish at 3 dpf and skeletal muscles were analyzed at 5 dpf as described previously [9]. Cardiotoxin administration resulted in an accumulation of a pool of muscle stem cells expressing Pax7 at the site of injury in control fish and efficient myofiber repair (Fig 4C). In contrast, ddx27 zebrafish muscle were composed of degenerating myofibers and no regeneration or muscle repair was observed (Fig 4C). These findings suggest that DDX27 plays a pivotal role in skeletal muscle regeneration by regulating the proliferation of muscle stem cells.

Nucleolar abnormalities and rRNA maturation defects in Ddx27 deficiency

Ddx27 is localized in the nucleolus that is primarily the site of ribosome biogenesis. Therefore, we evaluated nucleolar structure and functions to understand the impact of DDX27 on these processes in skeletal muscle. Immunofluorescence with different nucleolar markers showed changes in localization of the fibrillary component marker Ubf (labeling rRNA transcription sites) from small punctate foci to larger condensed areas, suggesting a perturbation in active transcription sites in the nucleolus. Similarly, fibrillarin-enriched dense fibrillary component areas of early rRNA-processing regions

were also disrupted and merged, forming larger, more condensed structures. Lastly, B23 distribution in the nucleolar granular component was drastically altered in the nucleoplasm (Fig. 5A). These results suggest that *Ddx27* deficiency disrupts both the sites of rRNA processing pathways and early ribosomal assembly. Analysis of rRNA transcription *in situ* by rRNA labeling of 5-EU in control and mutant zebrafish myofibers revealed a significant reduction in rRNA transcripts indicative of a defective rRNA transcription (Fig 6B).

Next, to evaluate the role of DDX27 on pre-rRNA processing in vertebrates, the pre-rRNA maturation pattern was evaluated in the skeletal muscle of *ddx27* mutant zebrafish by Northern blotting with different probes that were specific to various precursor rRNAs representing different pre-rRNA processing steps (Fig 5C). *ddx27* mutant skeletal muscle displayed significant accumulation of long pre-rRNAs (precursors A and B), corresponding to 47S and 43S pre-rRNAs in the human rRNA processing pathway. Precursors C (corresponding to human 32S pre-rRNA) also accumulated, while precursors to the 18S rRNA (precursors D, E, F) decreased. This accumulation of early precursors and of precursors C suggests an early defect in the rRNA maturation process and indicative of delayed cleavages in the 5'ETS and 3'ETS. These results are in accordance with recent data showing that depletion of DDX27 in human cells leads to the release of an extended form of the 47S primary transcript [32]. In addition, our data reveal an accumulation of 41S pre-rRNAs and a concomitant decrease of 30S pre-rRNAs, which are indicative of an impaired cleavage at site 2 (Fig 5C).

To study the impact of rRNA maturation defects on ribosomes, we performed ribosomal profiling in control and mutant zebrafish muscle that revealed a significant

decrease in free 60S large ribosomal subunits. A reduction of mature 80S monosomes as well as polysomes was also observed in mutant muscles (Fig 5D). Together these studies show that *ddx27* expression is required for the formation of mature rRNA species and thereby for biogenesis of functional polysomes in skeletal muscle.

Ddx27 deficiency perturbs the translation of specific subset of mRNA repertoires

We next sought to investigate if the ribosomal deficits due to Ddx27 deficiency affects global translation or a specific mRNA repertoire in skeletal muscle. Polysomes (actively translating ribosomes) were purified from control and *Ddx27* myoblasts. RNA-sequencing of total and polysome bound mRNA transcripts revealed that 124 transcripts that showed increased and 300 which showed decreased association with polysomes were common in both control and mutant. 1057 mRNA transcripts were exclusively enriched in control polysomes whereas *Ddx27* deficient polysomes showed an enrichment of 286 mRNA transcripts (Fig 6). Data analysis (Fig. S5-6) showed that control polysomes associated transcripts exhibited an enrichment in mRNAs encoding ribosomal, RNA polymerase, RNA degradation and splicing pathways suggesting a high requirement of these RNA metabolic processes during muscle cell growth. On the other hand, in Ddx27 deficiency an enrichment of apoptotic and inflammatory pathway genes was observed suggesting that absence of DDX27 perturbs the translation of mRNAs regulating RNA-metabolism and activates the atrophic processes in muscle. mRNAs regulating the atrophic/catabolic processes were significantly less enriched in polysomes in control skeletal muscles (e.g. amino acid degradation). In addition, mRNAs required for protein biosynthesis (amino acid biosynthesis, aminoacyl-tRNA biosynthesis) showed significantly lower enrichment in mutant polysomes. These result

suggest that DDX27 is crucial for the translation of mRNAs that are necessary for generating building blocks for active biosynthesis of proteins and suppression of transcripts associated with atrophic processes during muscle growth.

Interestingly, a number of signal transduction pathways associated with skeletal muscle growth and diseases are also perturbed in DDX27 deficiency. Mutant polysomes exhibited a reduced association with *Fgfr1* transcripts. FGF-signaling pathway is crucial for skeletal muscle development and muscle specific ablation of *Fgfr1* impairs proliferation of muscle satellite cells [33]. Additionally, an increase in mRNAs encoding members of MAP Kinase pathway that is associated with precocious differentiation was observed in *ddx27* mutant zebrafish muscles [34]. Lastly, we identified several novel mRNAs that were highly enriched in control polysomes but decreased in Ddx27-deficienct polysomes (e.g. *Ctsw*, *Hddc2*, *Tagln*, *Wfdc1 Sprr2h*, and *Vmn2r78*)(Fig 6C). Many of these genes are involved in the maintenance of proliferative state pf human ES and ipS cell however, their role/s in myogenesis are not known [35]. To confirmed the validity of our polysomal profiling data and expression of these transcripts in skeletal muscle we analyzed the expression of HDDC2 in control and *Ddx27* mutant myoblasts. Immunofluorescence and Western blotting revealed a significant downregulation of HDDC2 protein in *Ddx27* mutant myoblasts suggesting that HDDC2 may be contributing to DDX27 mediated muscle stem cell defects in skeletal muscle (Fig 6D). A reverse analysis also identified the downregulation of 4 novel transcripts in control myoblasts that were enriched in *Ddx27* polysomes, including *A330074K22Rik*, *Fhdc1*, *Gpr153*, and *Ston2* and future studies will be able to identify their functional roles in skeletal muscle. In sum, polysome profiling revealed that DDX27 is required for the translation of mRNAs regulating RNA metabolism and signaling pathway that are crucial for muscle satellite

cell proliferation and differentiation. In addition, we identified novel genes that are required for cellular proliferation and future studies on *in vivo* function of these genes in skeletal muscle development may help to understand novel processes regulating muscle growth.

Discussion

In this study, we hypothesized that *in vivo* identification of novel factors regulating myogenesis should help to elucidate the molecular mechanisms that regulate myogenic processes. Indeed, in this work we found that DDX27 regulates ribosome biogenesis and translational processes that in turn underlie muscle stem cell proliferation and skeletal muscle regeneration.

DDX27 belongs to the DEAD-box family of RNA helicases which represent a large protein family with 43 members that catalyze the ATP-dependent unwinding of double stranded RNA and variously function in remodeling structures of RNA or RNA/protein complexes, dissociating RNA/protein complexes, or RNA annealing [36]. Studies in yeast and cellular models have shown that several DDX family members regulate different steps of rRNA processing; however, *in vivo* functions of these RNA helicases during vertebrate development are still mostly unknown. While this plethora of RNA helicases implies the potential for functional redundancy, it also raises the attractive possibility that RNA helicases might perform a generic, unifying function in neuromuscular development by regulating RNA metabolism. DDX5/p68 RNA helicase promotes the assembly of proteins required for transcription initiation complex and chromatin remodeling during skeletal muscle differentiation [37]. Overexpression of *DDX5* also restores the skeletal muscle function in a mouse model of myotonic dystrophy [38]. RNA helicases (DDX1 and DDX3) play significant roles in muscle

development and disease by interacting with muscle specific transcription factors or with disease causing genes [39, 40].

We demonstrate that DDX27 is a nucleolar protein that localizes to muscle satellite cells. Although nucleolar proteins often have ubiquitous localization, the highly specialized sub-cellular expression of DDX27 and tissue-specific phenotypes in *Drosophila* suggests a specialized role for this protein. Consistent with this view, DDX27-deficient muscles exhibit disorganized sarcomeres and smaller myofibers. DDX27 deficiency also impairs the proliferation of Pax7-positive muscle stem cell population by the accumulation of cells at G1 stage of cell cycle. This critical role of DDX27 in regulating muscle stem cells was further supported by the impaired regeneration and absence of Pax7 expressing cells at the injury site in mutant fish. Concurrently, structural analysis and molecular markers suggest premature differentiation of skeletal muscle in Ddx27 deficiency potentially initiated by reduced Pax7 expression in the muscle stem cells in mutant muscle. While our polysomal profiling data did not identify PAX7 under the direct translational control of DDX27 regulated processes, we however, identified changes in enrichment of transcripts in mutant polysomes that encode members of FGF and MAPK signaling pathways. These signaling pathway are associated with activation and myogenic commitment of muscle stem cells and thus could be contributing to the skeletal muscle defects observed in DDx27 deficiency.

Molecularly, we establish that DDX27 regulates rRNA maturation and ribosome biogenesis. DDX27 is highly conserved in evolution, and mutation of the yeast *ddx27* ortholog, *drs1p*, results in 25S rRNA maturation and 60S ribosome subunit biogenesis defects [41]. In zebrafish and mammalian cells, we identified an accumulation of

primary transcripts and long-pre-rRNAs reflecting early rRNA maturation defects resulting in a decrease in functional ribosomes. Previous studies, have shown that ribosomes are increased during skeletal muscle hypertrophy and reduced in atrophied muscles or skeletal muscle diseases. However, the regulators of these processes remains to be identified. Our studies demonstrate that DDX27 is required for normal muscle growth by controlling rRNA maturation and ribosomal biogenesis. These work may have significant implications in regulating the myofiber size or slowing the degenerative processes in skeletal muscle diseases by targeting ribosomal biogenesis machinery. Polysomal profiling revealed an enrichment of transcripts regulating RNA metabolism pathways in control polysomes that was lacking in the mutant muscles. Defects in RNA metabolism underlie disease pathophysiology in a number of neuromuscular diseases [42]. Therefore, identification of critical regulators of RNA based processes in normal muscles is essential in order to understand the molecular basis of pathological changes in disease conditions. Our studies also identified abnormal association of transcripts associated with signal pathways that are crucial for muscle stem cell proliferation and myogenic commitment, such as FGF, and MAPK, are perturbed in *Ddx27* mutant myoblasts. Identification of these processes identifies an additional regulatory layer of translational regulation controlled by DDX27 that fine tunes the signal transduction pathways associated with skeletal muscle growth. Finally, we have identified a number of novel genes associated with cellular pluripotency and membrane remodeling that were previously not known to play any roles in skeletal muscle biology. Future work targeting these genes will help to illuminate additional processes that are crucial for myogenesis. The specificity of ribosomal changes and how they target translation of specific subsets of mRNAs remains open for further

investigation. This work provides new insight into nucleolar function in skeletal muscle development, and opens a new avenue to explore the specific roles of nucleolar proteins and ribosome biogenesis in development and disease.

EXPERIMENTAL PROCEDURES

Zebrafish lines

Fish were bred and maintained using standard methods as described (56). All procedures were approved by the Boston Children's Hospital Animal Care and Use Committee. Wild-type embryos were obtained from Oregon AB line and were staged by hours (h) or days (d) post fertilization at 28.58C.

Skeletal muscle regeneration

Cardiotoxin-induced muscle regeneration studies in zebrafish were performed following previously published protocols [43]. Briefly, control and *ddx27* mutant larvae (3 dpf) were anesthetized and immobilized by embedding into 3% low melting agarose. Cardiotoxin (10mM, 1 μl) was injected into dorsal somite muscles, and fish were analyzed at 5 dpf by immunofluorescence analysis. Muscle degeneration and regeneration in mice was performed as described previously [44].

Skeletal Muscle Functional Analysis

Functional experiments were performed as previously described [45]. Briefly, fish were studied in a bicarbonate buffer of the following composition: (in mM) 117.2 NaCl, 4.7 KCl, 1.2 $MgCl_2$, 1.2 KH_2PO_4, 2.5 $CaCl_2$, 25.2 $NaHCO_3$, 11.1 glucose (Dou et al., 2008). 4-5 dpf larvae were anesthetized in fish buffer containing 0.02% tricaine and

decapitated. The head tissue was used for genotyping. The larval body was transferred to a small chamber containing fish buffer equilibrated with 95% O_2, 5% CO_2 and maintained at 25 $^{\circ}$C. The larval body was attached to an isometric force transducer (Aurora Scientific, Aurora, Ontario, CAN, model 403A) and position motor (Aurora Scientific model 308B) using a 10-0 monofilament tie placed at the gastrointestinal opening and another tie attached several myotomes proximal from the tip of the tail. Twitches (200 μs pulse duration) and tetani (300 Hz) were elicited using supramaximal current delivered to platinum electrodes flanking the preparation. All data were collected at the optimal preparation length (L_o) for tetanic force. At the conclusion of the experiment, images of the preparations width and depth at L_o were obtained by carefully rotating the preparation about the gastrointestinal opening attachment point. Each image was analyzed by ImageJ using an internal length calibration. Preparation cross-sectional area (CSA) was calculated from width and depth measurements assuming the preparations cross-section was elliptical. Forces were calculated as active force, i.e. peak force minus the unstimulated baseline force, and are presented in absolute terms (valid because all larvae were attached at a consistent anatomical landmark, the gastrointestinal opening) as well as normalized to preparation CSA. The maximal rate of twitch tension development was determined as the maximal derivative of the force by time response between the onset of contraction and peak force. Likewise, the maximal rate of twitch tension relaxation was calculated as the first derivative of the force by time relaxation response, ranging from peak force until force had declined to approximately baseline. Statistical differences in the *ddx27* (n = 12) and control (n = 10) group means were evaluated by a two-sample t-test.

Single Myofiber culture and immunofluorescence

Wholemount immunofluorescence in zebrafish was performed as described previously (56). For immunofluorescence studies in zebrafish myofiber culture, previously published protocol was followed [46]. Paraformaldehyde (4%) or methanol (100%) were used as fixative for different antibodies. For C2C12 cells immunofluorescence, equal numbers of control and mutant cells were plated in chamber slides and incubated for at least 12-16 hours before performing immunofluorescence. Primary antibodies used in this study were: α-actinin (1:100; Sigma, A7811), RYR1 (1:100; Sigma, R-129), Fibrillarin (1:50; Santa Cruz, sc-25397), B23 (1:50; Santa Cruz, sc-5564), UBF (Sigma, 1:50, HPA006385), DDX27 (1:50, Santa Cruz, sc-81074), Pax7 (1:20; Developmental Studies Hybridoma Bank), Mef2 (1:20, Santa Cruz, sc-17785). For phalloidin staining, paraformaldehyde fixed embryos/larvae were incubated with phalloidin (1:40, Thermo Fisher Scientific, A12379) (and with primary antibody; for double immunofluorescence), overnight at 4°C followed by incubation with secondary antibody (if primary antibody was used). Nuclear staining was done using DAPI (Biolegend, 422801). Secondary antibodies (Thermo Fisher Scientific) were used between 1:100-1:250 dilutions.

rRNA transcription, maturation and ribosome analysis

rRNA transcription was detected using the Click-iT RNA Alexa Fluor imaging kit (C10329, Invitrogen) as described previously [47]. Briefly, to detect the synthesis of rRNAs in the nucleoplasm, control or *ddx27* knockout zebrafish myofibers were cultured in 8 chamber slides. Cells were treated with 1μg/mL actinomycin for 20 minutes and then incubated for 2 hours with 1mM 5-ethyl uridine (5-EU) in the presence or absence of actinomycin. The cells were fixed with paraformaldehyde (4%) and incubated with

Click-iT reaction cocktail for 1 hour. The cells were washed and DNA was counterstained with DAPI. The average 5-EU signal intensity in the nucleoplasm was measured from 20 nuclei per experiment using the ImageJ program. The level of rRNA was determined by actinomycin-treated and non-treated cells in control and mutant myofibers.

In order to analyze the precursors to the 28S and 18S rRNAs, total RNA samples were separated on a 1.2% agarose gel containing 1.2% formaldehyde and 1× Tri/Tri buffer (30 mM triethanolamine, 30 mM tricine, pH 7.9). RNAs were transferred to Hybond N^+ nylon membrane (GE Healthcare, Orsay, France) and cross-linked under UV light. Membrane hybridization with radiolabeled oligonucleotide probes was performed as described (Preti, 2013). Signals were acquired with a Typhoon Trio PhosphorImager and quantified using the MultiGauge software. The human probes were: 5'-TTTACTTCCTCTAGATAGTCAAGTTCGACC-3' (18S), 5'-CCTCGCCCTCCGGGCTCCGTTAATGATC-3' (5'ITS1), a mixture of 5'-CTGCGAGGGAACCCCCAGCCGCGCA-3' (ITS2-1) and 5'-GCGCGACGGCGGACGACACCGCGGCGTC-3' (ITS2-2), 5'-CCCGTTCCCTTGGCTGTGGTTTCGCTAGATA-3' (28S), 5'-GCACGCGCGCGCGGACAAACCCTTG-3' (28S-3'ETS). The zebrafish probes were: 5'-GAGGGAGGCGCGTCGACCTTCGCTGGGC-3' (3'ETS), 5'-CAGCTTTGCAACCATACTCCCCCCGGAAC-3' (18S), 5'-GAGATCCCCTCTCGAACCCGTAATGAT-3' (ITS1), 5'-GAGCGCTGGCCTCGGAGATCGCTGGGTCGC-3' (ITS2), 5'-CCTCTCGTACTGAGCAGGATTACTATTGC-3' (28S). For ribosome profile analysis zebrafish myofibers were treated with cycloheximide (Sigma, 100ug/ML) in

differentiation media (DMEM + 2% horse serum) for 10 minutes at room temperature. Subsequently, myofibers were flash frozen in liquid nitrogen in lysis buffer (10mM Tris-Cl, pH 7.4, 5mM MgCl2, 100mM KCl, 1% TritonX-100). To purify ribosomal fractions, cell lysate (0.75 ml) was layered on 10-50% sucrose gradient and centrifuged at 36,000 rpm using SW-41 Ti rotor, 2 hours at 4°C. The fractions were collected and were analyzed at 254nm.

Polysomal profiling

Polysome ribosome fractions prepared as described above were pooled together, treated with proteinase K and RNA was isolated using acid phenol-chloroform extraction and ethanol precipitation. Deep sequencing libraries were generated and sequenced as described [48]. Splice-Aware alignment program STAR was used to map sequencing reads to *Mus musculus* (mm10 build). R package "edgeR" was employed to identify differential gene expression calls from these sequence reads. Gene expression was considered to be up-regulated if log2FC> +1 or downregulated if the log2FC< -1 (FC=fold change of average CPM) with respect to the condition being compared at a false discovery rate <0.05. Functional ontological classification of different gene lists was performed by DAVID .

Proliferation and apoptosis Assays

To analyze the proliferating cells in C2C12 cell cultures and zebrafish embryos, Edu labeling was performed. For zebrafish, embryos (48 hrs) were placed in 1mL of 500μM EdU/10% DMSO in E3 media and incubated on ice for 2 h. Embryos were transferred back to the incubator at 28.5 °C and samples were collected at desired time intervals

and fixed with paraformaldehyde (4%), followed by fixation in methanol (-20°C, 10 mins). Fish were permeabilized with 1% tritonX-100/PBS for 1 hr and Click-iT reaction cocktail (Thermo Fisher Scientific) was added and incubated in dark for 1 hr at room temperature, washed and analyzed by confocal microscopy. For analyzing proliferating C2C12 cells, equal number of control and mutant cells (to 40-50% confluency) were plated for 12-14 hours. 2X EdU solution was added to the cells and incubated for 2 hrs at 37°C. After incubation cells were permeabilized with 0.5% triton-100 and labeled with Click-iT reaction cocktail as described for zebrafish. Immunofluorescence was performed with Pax7 antibody (DHSB) and nuclei were stained with DAPI.

Detailed experimental details are provided in the supplemental material.

AUTHOR CONTRIBUTIONS

Conceptualization V.A.G.; and A.H.B.[1]; Methodology, V.A.G.; M.F.O.; J.W.; I.D.; A.C.; and Y.Z., Investigation, A.H.B.[2]; M.F.O; S.R.G; A.T.C; J.W.; I.D.; and V.A.G.; Writing-Original Draft, V.A.G.; and A.H.B.[2]; Writing- Review & Editing, M.F.O.; J.W.; I.D.; P-E.G.; A.H.B.[1]; and V.A.G., Funding Acquisition, V.A.G.; A.H.B.[1]; L.I.Z.; and P-E.G.; Resources, A.H.B.[1]; L.I.Z.; and V.A.G.; Supervision, A.H.B.[1]; and V.A.G.

A.H.B.[1]; Alan H Beggs

A.H.B.[2]; Alexis H Bennett

Acknowledgements

VAG is supported by K01 AR062601 from the National Institute of Arthritis and Musculoskeletal and Skin Diseases of National Institute of Health. This work was

supported by the Eleanor and Miles Shore Fellowship for Scholars in Medicine and Brigham and Women's Hospital Career development award (VAG), a Charles H Hood Foundation Child Health Research Grant (VAG), Muscular Dystrophy Association of USA grant (MDA383249, AHB), National Institutes of Health grants from the National Institute of Arthritis and Musculoskeletal and Skin Diseases R01 (AR044345, AHB), National Heart, Lung and Blood Institute (U01 HL100001, LIZ) and Office of the Director (R24 OD017870, LIZ). PEG and MFO are supported by the CNRS, the University of Toulouse-Paul Sabatier and a grant of the Agence Nationale de la Recherche (ANR15-CE12-0001-02). The authors are grateful to Nathalie Montel-Lehry for technical support with rRNA analyses.

REFERENCES

1. Tafforeau L, Zorbas C, Langhendries JL, Mullineux ST, Stamatopoulou V, Mullier R, et al. The complexity of human ribosome biogenesis revealed by systematic nucleolar screening of Pre-rRNA processing factors. Mol Cell. 2013;51(4):539-51. doi: 10.1016/j.molcel.2013.08.011. PubMed PMID: 23973377.
2. Buszczak M, Signer RA, Morrison SJ. Cellular differences in protein synthesis regulate tissue homeostasis. Cell. 2014;159(2):242-51. doi: 10.1016/j.cell.2014.09.016. PubMed PMID: 25303523; PubMed Central PMCID: PMCPMC4222182.
3. Slavov N, Semrau S, Airoldi E, Budnik B, van Oudenaarden A. Differential Stoichiometry among Core Ribosomal Proteins. Cell Rep. 2015;13(5):865-73. doi: 10.1016/j.celrep.2015.09.056. PubMed PMID: 26565899; PubMed Central PMCID: PMCPMC4644233.
4. You KT, Park J, Kim VN. Role of the small subunit processome in the maintenance of pluripotent stem cells. Genes Dev. 2015;29(19):2004-9. doi: 10.1101/gad.267112.115. PubMed PMID: 26443847; PubMed Central PMCID: PMCPMC4604342.
5. Shi Z, Barna M. Translating the genome in time and space: specialized ribosomes, RNA regulons, and RNA-binding proteins. Annu Rev Cell Dev Biol. 2015;31:31-54. doi: 10.1146/annurev-cellbio-100814-125346. PubMed PMID: 26443190.
6. Dumont NA, Wang YX, Rudnicki MA. Intrinsic and extrinsic mechanisms regulating satellite cell function. Development. 2015;142(9):1572-81. doi: 10.1242/dev.114223. PubMed PMID: 25922523; PubMed Central PMCID: PMCPMC4419274.

7. Bentzinger CF, Wang YX, Rudnicki MA. Building muscle: molecular regulation of myogenesis. Cold Spring Harb Perspect Biol. 2012;4(2). doi: 10.1101/cshperspect.a008342. PubMed PMID: 22300977; PubMed Central PMCID: PMCPMC3281568.
8. Seger C, Hargrave M, Wang X, Chai RJ, Elworthy S, Ingham PW. Analysis of Pax7 expressing myogenic cells in zebrafish muscle development, injury, and models of disease. Dev Dyn. 2011;240(11):2440-51. doi: 10.1002/dvdy.22745. PubMed PMID: 21954137.
9. Gurevich DB, Nguyen PD, Siegel AL, Ehrlich OV, Sonntag C, Phan JM, et al. Asymmetric division of clonal muscle stem cells coordinates muscle regeneration in vivo. Science. 2016;353(6295):aad9969. doi: 10.1126/science.aad9969. PubMed PMID: 27198673.
10. Conboy MJ, Karasov AO, Rando TA. High incidence of non-random template strand segregation and asymmetric fate determination in dividing stem cells and their progeny. PLoS Biol. 2007;5(5):e102. doi: 10.1371/journal.pbio.0050102. PubMed PMID: 17439301; PubMed Central PMCID: PMCPMC1852584.
11. Sohn RL, Huang P, Kawahara G, Mitchell M, Guyon J, Kalluri R, et al. A role for nephrin, a renal protein, in vertebrate skeletal muscle cell fusion. Proc Natl Acad Sci U S A. 2009;106(23):9274-9. doi: 10.1073/pnas.0904398106. PubMed PMID: 19470472; PubMed Central PMCID: PMCPMC2695070.
12. Millay DP, Sutherland LB, Bassel-Duby R, Olson EN. Myomaker is essential for muscle regeneration. Genes Dev. 2014;28(15):1641-6. doi: 10.1101/gad.247205.114. PubMed PMID: 25085416; PubMed Central PMCID: PMCPMC4117939.
13. Gupta VA, Ravenscroft G, Shaheen R, Todd EJ, Swanson LC, Shiina M, et al. Identification of KLHL41 Mutations Implicates BTB-Kelch-Mediated Ubiquitination as an Alternate Pathway to Myofibrillar Disruption in Nemaline Myopathy. Am J Hum Genet. 2013;93(6):1108-17. doi: 10.1016/j.ajhg.2013.10.020. PubMed PMID: 24268659; PubMed Central PMCID: PMCPMC3852928.
14. Marabita M, Baraldo M, Solagna F, Ceelen JJ, Sartori R, Nolte H, et al. S6K1 Is Required for Increasing Skeletal Muscle Force during Hypertrophy. Cell Rep. 2016;17(2):501-13. doi: 10.1016/j.celrep.2016.09.020. PubMed PMID: 27705797.
15. Wen Y, Alimov AP, McCarthy JJ. Ribosome Biogenesis is Necessary for Skeletal Muscle Hypertrophy. Exerc Sport Sci Rev. 2016;44(3):110-5. doi: 10.1249/JES.0000000000000082. PubMed PMID: 27135313; PubMed Central PMCID: PMCPMC4911282.
16. Chaillou T, Kirby TJ, McCarthy JJ. Ribosome biogenesis: emerging evidence for a central role in the regulation of skeletal muscle mass. J Cell Physiol. 2014;229(11):1584-94. doi: 10.1002/jcp.24604. PubMed PMID: 24604615; PubMed Central PMCID: PMCPMC4868551.
17. Poche H, Schulze H. Ribosomal protein synthesis in cultured skin fibroblast cells obtained from patients with Duchenne muscular dystrophy. J Neurol Sci. 1985;70(3):295-304. PubMed PMID: 4056825.
18. Jolicoeur C, Noel J, Brakier-Gingras L. The 60S ribosomal subunit is altered in the skeletal muscle of dystrophic hamsters. Biochem Biophys Res Commun. 1983;115(1):153-8. PubMed PMID: 6615523.
19. Ohanna M, Sobering AK, Lapointe T, Lorenzo L, Praud C, Petroulakis E, et al. Atrophy of S6K1(-/-) skeletal muscle cells reveals distinct mTOR effectors for cell cycle

and size control. Nat Cell Biol. 2005;7(3):286-94. doi: 10.1038/ncb1231. PubMed PMID: 15723049.
20. Ionasescu V. Distinction between Duchenne and other muscular dystrophies by ribosomal protein synthesis. J Med Genet. 1975;12(1):49-54. PubMed PMID: 164552; PubMed Central PMCID: PMCPMC1013230.
21. Machida M, Takeda K, Yokono H, Ikemune S, Taniguchi Y, Kiyosawa H, et al. Reduction of ribosome biogenesis with activation of the mTOR pathway in denervated atrophic muscle. J Cell Physiol. 2012;227(4):1569-76. doi: 10.1002/jcp.22871. PubMed PMID: 21678406.
22. Gupta V, Kawahara G, Gundry SR, Chen AT, Lencer WI, Zhou Y, et al. The zebrafish dag1 mutant: a novel genetic model for dystroglycanopathies. Hum Mol Genet. 2011;20(9):1712-25. doi: 10.1093/hmg/ddr047. PubMed PMID: 21296866; PubMed Central PMCID: PMCPMC3071669.
23. Gupta VA, Kawahara G, Myers JA, Chen AT, Hall TE, Manzini MC, et al. A splice site mutation in laminin-alpha2 results in a severe muscular dystrophy and growth abnormalities in zebrafish. PLoS One. 2012;7(8):e43794. doi: 10.1371/journal.pone.0043794. PubMed PMID: 22952766; PubMed Central PMCID: PMCPMC3428294.
24. Ochi H, Westerfield M. Signaling networks that regulate muscle development: lessons from zebrafish. Dev Growth Differ. 2007;49(1):1-11. doi: 10.1111/j.1440-169X.2007.00905.x. PubMed PMID: 17227340.
25. Brand AH, Perrimon N. Targeted gene expression as a means of altering cell fates and generating dominant phenotypes. Development. 1993;118(2):401-15. PubMed PMID: 8223268.
26. Carpenter S, Karpati, G. Pathology of Skeletal Muscle. 2nd ed. New York: Oxford University press; 2001. 704 p.
27. Bassett DI, Bryson-Richardson RJ, Daggett DF, Gautier P, Keenan DG, Currie PD. Dystrophin is required for the formation of stable muscle attachments in the zebrafish embryo. Development. 2003;130(23):5851-60. doi: 10.1242/dev.00799. PubMed PMID: 14573513.
28. Ishibashi J, Perry RL, Asakura A, Rudnicki MA. MyoD induces myogenic differentiation through cooperation of its NH2- and COOH-terminal regions. J Cell Biol. 2005;171(3):471-82. doi: 10.1083/jcb.200502101. PubMed PMID: 16275751; PubMed Central PMCID: PMCPMC2171269.
29. Olguin HC, Pisconti A. Marking the tempo for myogenesis: Pax7 and the regulation of muscle stem cell fate decisions. J Cell Mol Med. 2012;16(5):1013-25. doi: 10.1111/j.1582-4934.2011.01348.x. PubMed PMID: 21615681; PubMed Central PMCID: PMCPMC4365881.
30. Olguin HC, Yang Z, Tapscott SJ, Olwin BB. Reciprocal inhibition between Pax7 and muscle regulatory factors modulates myogenic cell fate determination. J Cell Biol. 2007;177(5):769-79. doi: 10.1083/jcb.200608122. PubMed PMID: 17548510; PubMed Central PMCID: PMCPMC2064278.
31. Gurevich D, Siegel A, Currie PD. Skeletal myogenesis in the zebrafish and its implications for muscle disease modelling. Results Probl Cell Differ. 2015;56:49-76. doi: 10.1007/978-3-662-44608-9_3. PubMed PMID: 25344666.
32. Kellner M, Rohrmoser M, Forne I, Voss K, Burger K, Muhl B, et al. DEAD-box helicase DDX27 regulates 3' end formation of ribosomal 47S RNA and stably associates

with the PeBoW-complex. Exp Cell Res. 2015;334(1):146-59. doi: 10.1016/j.yexcr.2015.03.017. PubMed PMID: 25825154.
33. Yablonka-Reuveni Z, Danoviz ME, Phelps M, Stuelsatz P. Myogenic-specific ablation of Fgfr1 impairs FGF2-mediated proliferation of satellite cells at the myofiber niche but does not abolish the capacity for muscle regeneration. Front Aging Neurosci. 2015;7:85. doi: 10.3389/fnagi.2015.00085. PubMed PMID: 26074812; PubMed Central PMCID: PMCPMC4446549.
34. Shi H, Boadu E, Mercan F, Le AM, Flach RJ, Zhang L, et al. MAP kinase phosphatase-1 deficiency impairs skeletal muscle regeneration and exacerbates muscular dystrophy. FASEB J. 2010;24(8):2985-97. doi: 10.1096/fj.09-150045. PubMed PMID: 20371627; PubMed Central PMCID: PMCPMC2909286.
35. Hasegawa Y, Taylor D, Ovchinnikov DA, Wolvetang EJ, de Torrente L, Mar JC. Variability of Gene Expression Identifies Transcriptional Regulators of Early Human Embryonic Development. PLoS Genet. 2015;11(8):e1005428. doi: 10.1371/journal.pgen.1005428. PubMed PMID: 26288249; PubMed Central PMCID: PMCPMC4546122.
36. Linder P, Jankowsky E. From unwinding to clamping - the DEAD box RNA helicase family. Nat Rev Mol Cell Biol. 2011;12(8):505-16. doi: 10.1038/nrm3154. PubMed PMID: 21779027.
37. Caretti G, Schiltz RL, Dilworth FJ, Di Padova M, Zhao P, Ogryzko V, et al. The RNA helicases p68/p72 and the noncoding RNA SRA are coregulators of MyoD and skeletal muscle differentiation. Dev Cell. 2006;11(4):547-60. doi: 10.1016/j.devcel.2006.08.003. PubMed PMID: 17011493.
38. Jones K, Wei C, Schoser B, Meola G, Timchenko N, Timchenko L. Reduction of toxic RNAs in myotonic dystrophies type 1 and type 2 by the RNA helicase p68/DDX5. Proc Natl Acad Sci U S A. 2015;112(26):8041-5. doi: 10.1073/pnas.1422273112. PubMed PMID: 26080402; PubMed Central PMCID: PMCPMC4491770.
39. Onishi H, Kino Y, Morita T, Futai E, Sasagawa N, Ishiura S. MBNL1 associates with YB-1 in cytoplasmic stress granules. J Neurosci Res. 2008;86(9):1994-2002. doi: 10.1002/jnr.21655. PubMed PMID: 18335541.
40. Ravel-Chapuis A, Klein Gunnewiek A, Belanger G, Crawford Parks TE, Cote J, Jasmin BJ. Staufen1 impairs stress granule formation in skeletal muscle cells from myotonic dystrophy type 1 patients. Mol Biol Cell. 2016;27(11):1728-39. doi: 10.1091/mbc.E15-06-0356. PubMed PMID: 27030674; PubMed Central PMCID: PMCPMC4884064.
41. Ripmaster TL, Vaughn GP, Woolford JL, Jr. A putative ATP-dependent RNA helicase involved in Saccharomyces cerevisiae ribosome assembly. Proc Natl Acad Sci U S A. 1992;89(23):11131-5. PubMed PMID: 1454790; PubMed Central PMCID: PMCPMC50503.
42. Ranum LP, Cooper TA. RNA-mediated neuromuscular disorders. Annu Rev Neurosci. 2006;29:259-77. doi: 10.1146/annurev.neuro.29.051605.113014. PubMed PMID: 16776586.
43. Li YH, Chen HY, Li YW, Wu SY, Wangta L, Lin GH, et al. Progranulin regulates zebrafish muscle growth and regeneration through maintaining the pool of myogenic progenitor cells. Sci Rep. 2013;3:1176. doi: 10.1038/srep01176. PubMed PMID: 23378909; PubMed Central PMCID: PMCPMC3560382.
44. Alexander MS, Casar JC, Motohashi N, Vieira NM, Eisenberg I, Marshall JL, et al. MicroRNA-486-dependent modulation of DOCK3/PTEN/AKT signaling pathways

improves muscular dystrophy-associated symptoms. J Clin Invest. 2014;124(6):2651-67. doi: 10.1172/JCI73579. PubMed PMID: 24789910; PubMed Central PMCID: PMCPMC4038577.
45. Widrick JJ, Alexander M, Sanchez B, Gibbs D, Kawahara G, Beggs A, et al. Muscle dysfunction in a zebrafish model of Duchenne muscular dystrophy. Physiol Genomics. 2016:physiolgenomics 00088 2016. doi: 10.1152/physiolgenomics.00088.2016. PubMed PMID: 27764767.
46. Smith LL, Gupta VA, Beggs AH. Bridging integrator 1 (Bin1) deficiency in zebrafish results in centronuclear myopathy. Hum Mol Genet. 2014;23(13):3566-78. doi: 10.1093/hmg/ddu067. PubMed PMID: 24549043; PubMed Central PMCID: PMCPMC4049309.
47. Lin T, Meng L, Lin TC, Wu LJ, Pederson T, Tsai RY. Nucleostemin and GNL3L exercise distinct functions in genome protection and ribosome synthesis, respectively. J Cell Sci. 2014;127(Pt 10):2302-12. doi: 10.1242/jcs.143842. PubMed PMID: 24610951.
48. Bukhari SI, Truesdell SS, Lee S, Kollu S, Classon A, Boukhali M, et al. A Specialized Mechanism of Translation Mediated by FXR1a-Associated MicroRNP in Cellular Quiescence. Mol Cell. 2016;61(5):760-73. doi: 10.1016/j.molcel.2016.02.013. PubMed PMID: 26942679; PubMed Central PMCID: PMCPMC4811377.

FIGURE LEGENDS

Figure 1. Mutation in a nucleolar protein *ddx27* results in skeletal muscle abnormalities

(A) Microscopic visualization of control and mutant larval zebrafish (*osoi*) at 5 days post fertilization (dpf). Mutant fish display leaner muscles (left panel) and exhibit highly reduced birefringence in comparison to control (right panel). Mutant fish also exhibit pericardial edema (arrow)

(B) Genetic mapping of *osoi* mutant by initial bulk segregant analysis identified linkage on chromosome 6. Fine mapping of chromosome 6 resolved flanking markers z41548 and z14467, with a candidate genome region containing six candidate genes that were sequenced by Sanger sequencing

(C) Immunofluorescence analysis of adult human skeletal muscle (quadriceps) revealed expression of DDX27 in PAX positive nuclei (scale bar: 50μm)

(D) Real-time PCR showing expression of *Ddx27* during skeletal muscle regeneration. TA muscle was injected with cardiotoxin or PBS and was harvested at day 7. Data is normalized to *Gapdh*. Data are presented as mean ± SEM. n=3 for each time point.

(E) Schematic diagram of nucleolus depicting nucleolar domains. Eukaryotic nucleolus has tripartite architecture: Fibrillar center (FC); Dense fibrillar component (DFC) and granular compartment (GC). Immunofluorescence of human myoblasts with DDX27 and nucleolar markers labeling each compartment of nucleolus (scale bar: 2μm)

Figure 2. Ddx27 deficiency results in skeletal muscle hypotrophy and precocious differentiation.

(A-B) Histology of longitudinal skeletal muscle sections in control and *ddx27* mutant stained with toluidine blue exhibiting enlarged nuclei (arrowhead) and areas lacking sarcomeres (arrow) at 5 dpf. High magnification view (boxed area)
(C-G) Transmission electron micrographs of skeletal muscles (longitudinal view: C-E, and cross-section view: F-G) in control and *ddx27* mutant (5 dpf). Arrows indicating disorganized sarcomere
(H) Quantification of myofiber size in control and *ddx27* mutant fish (5 dpf) (n=10)
(I) qRT-PCR of control and *ddx27* mutant fish showed a reduction in the expression of muscle stem cell markers (*pax3*, *pax7*) and an increase in expression of myogenic commitment genes (*myod1* and *myf5*). The expression of late differentiation markers was reduced in *ddx27* fish suggesting that pre-maturation expression of early myogenic genes results in abnormal disorganization of skeletal muscles.

Figure 3. Ddx27 skeletal muscle produce decreased contractile force and prolonged muscle relaxation.
(A) Representative twitch (left) and tetanic force (right) records from control and *ddx26* zebrafish (5 dpf) preparation
(B) Peak tetanic force
(C) Peak tetanic force normalized to preparation cross-sectional area. Tetanic force is significantly reduced in *ddx27* mutant fish
(D) Peak twitch force
(E) Peak twitch force normalized to preparation cross-sectional area. Twitch force is significantly reduced in *ddx27* mutant fish
(F) Maximal rate of twitch tension development.
(G) Maximum rate of twitch force relaxation.
(H) Twitch to tetanic force ratio.
Each symbol represents an individual control (n = 10) or *ddx27* (n = 12) preparation with the group mean indicated by a horizontal line. t-tests indicated significant differences between control and mutant means for all 7 variables ($P < 0.001$ to $P < 0.0001$).
Abbreviations: CSA, cross-sectional area; +dP/dt, maximal rate of tension development; -dP/dt, maximal rate of tension relaxation; Pt, peak twitch force; Po, peak tetanic force.

Figure 4. Ddx27 deficiency results in a decrease in number of muscle stem cell proliferation and regeneration
(A) Whole mount immunofluorescence of zebrafish at different time intervals (2 dpf and 4 dpf) with muscle stem cell marker (Pax7) and late differentiation marker (Mef2) demonstrating a decrease in of muscle stem cells in *ddx27* mutant during post-embryonic skeletal muscle growth (4 dpf) (scale bar: 50μm)
(B) Control and *ddx27* mutant zebrafish were pulse-labeled with EdU for 2hr and analyzed for EdU labeling (4 dpf) by whole mount immunofluorescence in zebrafish dermomyotome containing muscle satellite cells. Nuclei were stained with DAPI (scale bar: 50μm)
(C) Trunk muscles in control and *ddx27* zebrafish were injected with cardiotoxin (3 dpf). Skeletal muscles were analyzed at 5 dpf by whole mount immunofluorescence with Pax7 and phalloidin. Control muscles show an accumulation of Pax7 expressing cells at the site of injury (arrow) that was lacking in *ddx27* muscles (arrow) (scale bar: 50μm)

Figure 5. Ddx27 deficiency disrupts nucleolar architecture and rRNA synthesis resulting in ribosomal defects

(A) Immunofluorescence of cultured myofibers from control and *ddx27* mutant fish with antibodies labeling different nucleolar compartments at 5 dpf (scale bar: 10μm)

(B) rRNA transcription was measured in cultured myofibers at 5 dpf by quantifying the incorporation of 5-ethynl uridine (5-EU). Cells were treated with Actinomycin D for two hours to block background transcription. Subsequently, cells were incubated with or without Actinomycin D and freshly synthesized rRNA was quantified by incorporation of 5-EU by fluorescent detection (scale bar: 5μm)

(C) Northern blot analysis of total RNAs extracted from control and mutant ddx27 zebrafish larvae (5 dpf). 5'ETS, 5'ITS1 and ITS2 probes were used to identify pre-rRNA and intermediate species targeted different steps of the processing pathways. The pre-rRNA intermediates are described in zebrafish. The corresponding human precursors are indicated into brackets.

(D) Polysomal profiles of control and *ddx27* mutant larvae (5 dpf).

Figure 6. Ddx27 is required to regulate specific mRNA repertories in skeletal muscle.

(A)Polysomal profiling and RNA sequencing of total cellular mRNA transcripts and polysomal fractions were performed in control and *Ddx27* mutant myoblasts.

(B) mRNAs transcripts exhibiting expression values of Log_2Fold change >+1 were considered upregulated and those displaying Log_2Fold change <+1 were considered downregulated in the polysomal fraction in comparison to total cellular mRNA. Upregulated and downregulated mRNAs populations in control and *Ddx27* myoblasts were compared

(C) Expression of mRNA transcripts exhibiting maximum differences in control and Ddx27 mutant myoblasts

(D) Immunofluorescence and Western blot quantification of HDDC2 expression in control and *Ddx27* proliferating myoblasts (scale bar: 100μm).

Figure 1

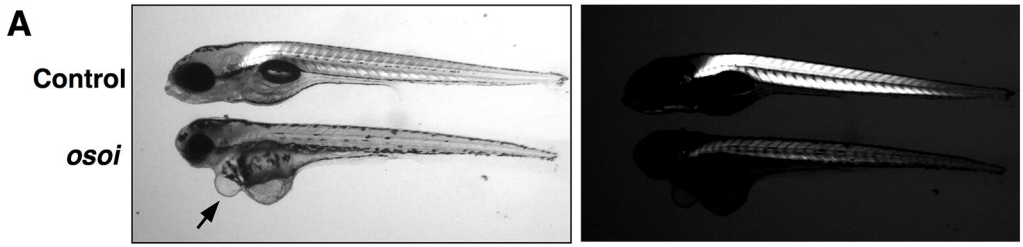
A
Control
osoi

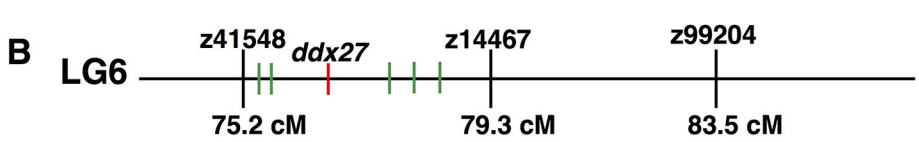
B
LG6
z41548
ddx27
z14467
z99204
75.2 cM
79.3 cM
83.5 cM

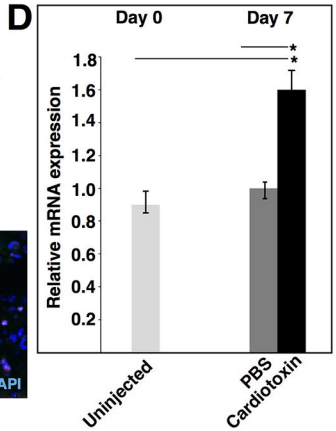
D
Day 0
Day 7
Relative mRNA expression
1.8
1.6
1.4
1.2
1.0
0.8
0.6
0.4
0.2
Uninjected
PBS
Cardiotoxin

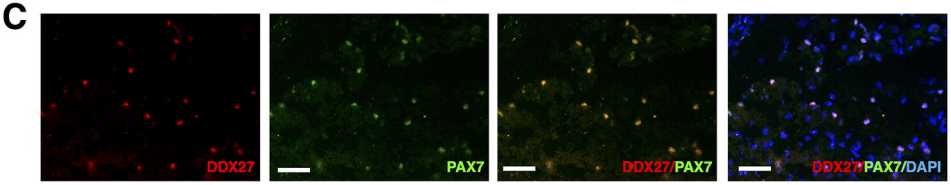
C
DDX27
PAX7
DDX27/PAX7
DDX27/PAX7/DAPI

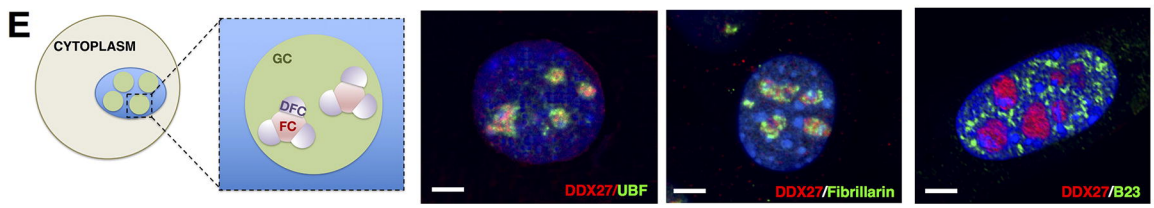
E
CYTOPLASM
GC
DFC
FC
DDX27/UBF
DDX27/Fibrillarin
DDX27/B23

Figure 2

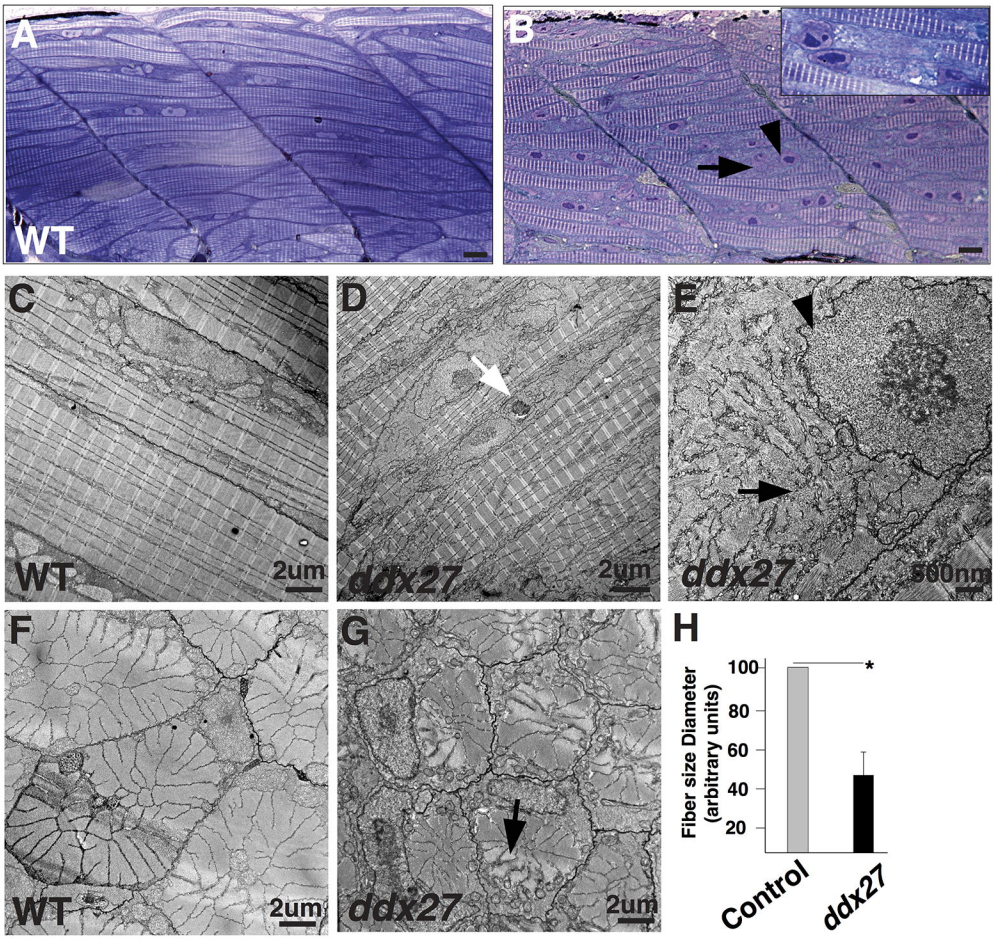
A
WT
B
C
WT
2um
D
ddx27
2um
E
ddx27
500nm
F
WT
2um
G
ddx27
2um
H
Fiber size Diameter (arbitrary units)
100
80
60
40
20
*
Control
ddx27
I
mRNA expression (arbitrary units)
Control 2 dpf
Control 4 dpf
ddx27 2 dpf
ddx27 4 dpf
1.8
1.6
1.4
1.2
1.0
0.8
0.6
0.4
0.2
pax3a
pax3b
pax7a
pax7b
myod1
myf5
myog
mylz
des

Figure. 3

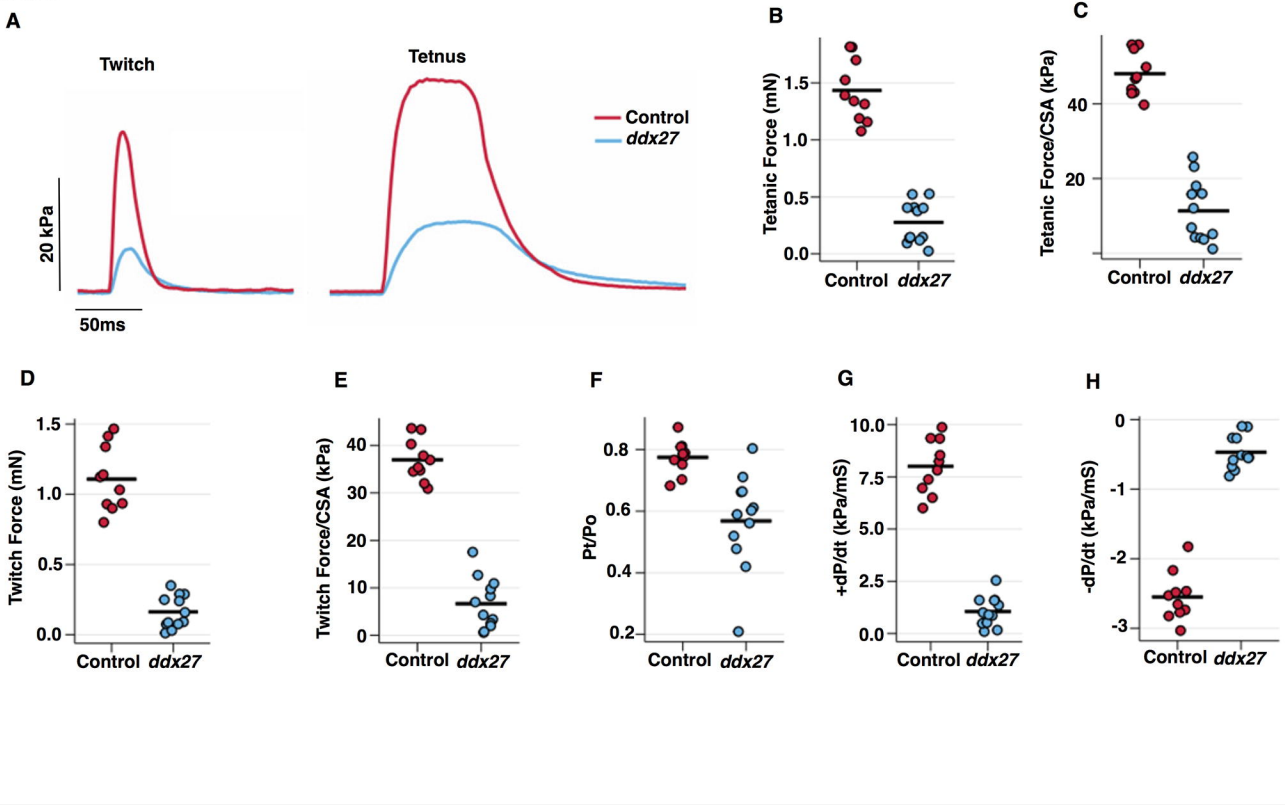
A
Twitch
Tetnus
Control
ddx27
20 kPa
50ms
B
Tetanic Force (mN)
1.5
1.0
0.5
0.0
Control
ddx27
C
Tetanic Force/CSA (kPa)
40
20
Control
ddx27
D
Twitch Force (mN)
1.5
1.0
0.5
0.0
Control
ddx27
E
Twitch Force/CSA (kPa)
40
30
20
10
0
Control
ddx27
F
Pt/Po
0.8
0.6
0.4
0.2
Control
ddx27
G
+dP/dt (kPa/mS)
10.0
7.5
5.0
2.5
0.0
Control
ddx27
H
-dP/dt (kPa/mS)
0
-1
-2
-3
Control
ddx27

Figure 4

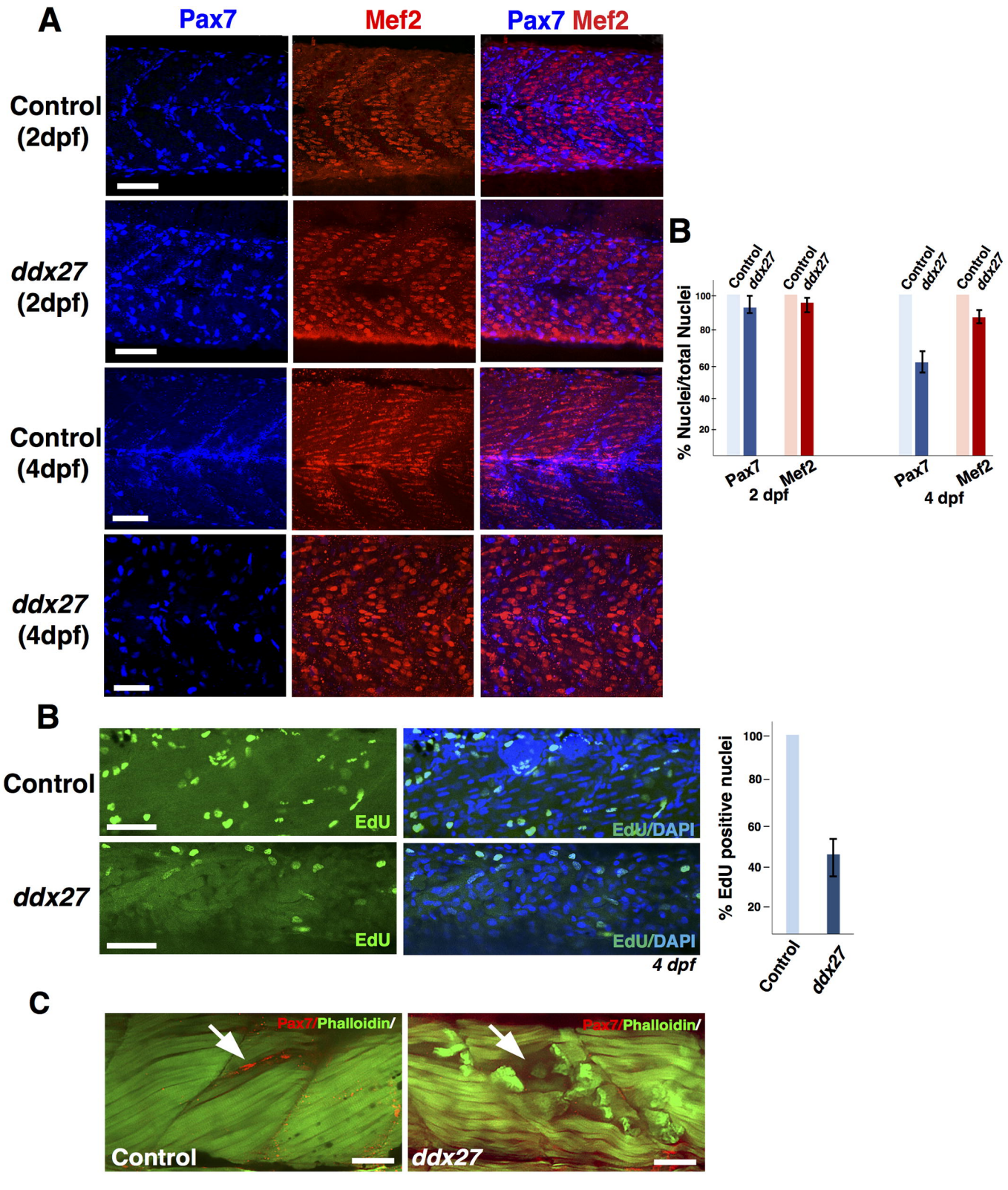
A
Pax7
Mef2
Pax7 Mef2
Control (2dpf)
ddx27 (2dpf)
Control (4dpf)
ddx27 (4dpf)
B
Control
ddx27
Control
ddx27
% Nuclei/total Nuclei
100
80
60
40
20
Pax7
Mef2
2 dpf
Pax7
Mef2
4 dpf
B
Control
ddx27
EdU
EdU/DAPI
EdU
EdU/DAPI
4 dpf
% EdU positive nuclei
100
80
60
40
20
Control
ddx27
C
Pax7/Phalloidin/
Pax7/Phalloidin/
Control
ddx27

Figure 5

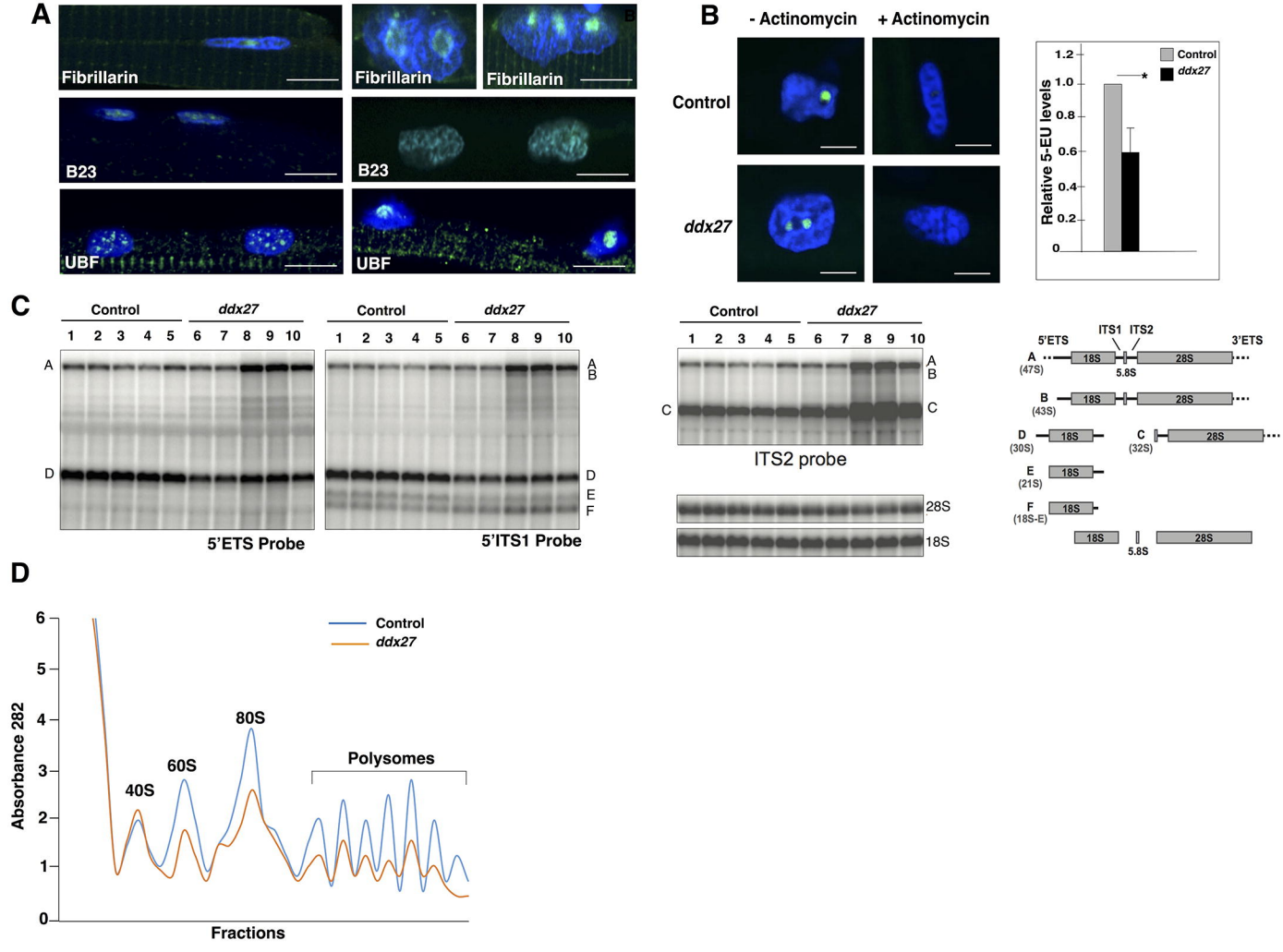
A
Fibrillarin
Fibrillarin
Fibrillarin
B23
B23
UBF
UBF
B
- Actinomycin
+ Actinomycin
Control
ddx27
Relative 5-EU levels
Control
ddx27
C
Control
ddx27
1 2 3 4 5 6 7 8 9 10
A
D
5'ETS Probe
5'ITS1 Probe
ITS2 probe
28S
18S
5'ETS
ITS1
ITS2
3'ETS
18S
28S
5.8S
(47S)
(43S)
(30S)
(32S)
(21S)
(18S-E)
D
Absorbance 282
Fractions
40S
60S
80S
Polysomes

Figure 6

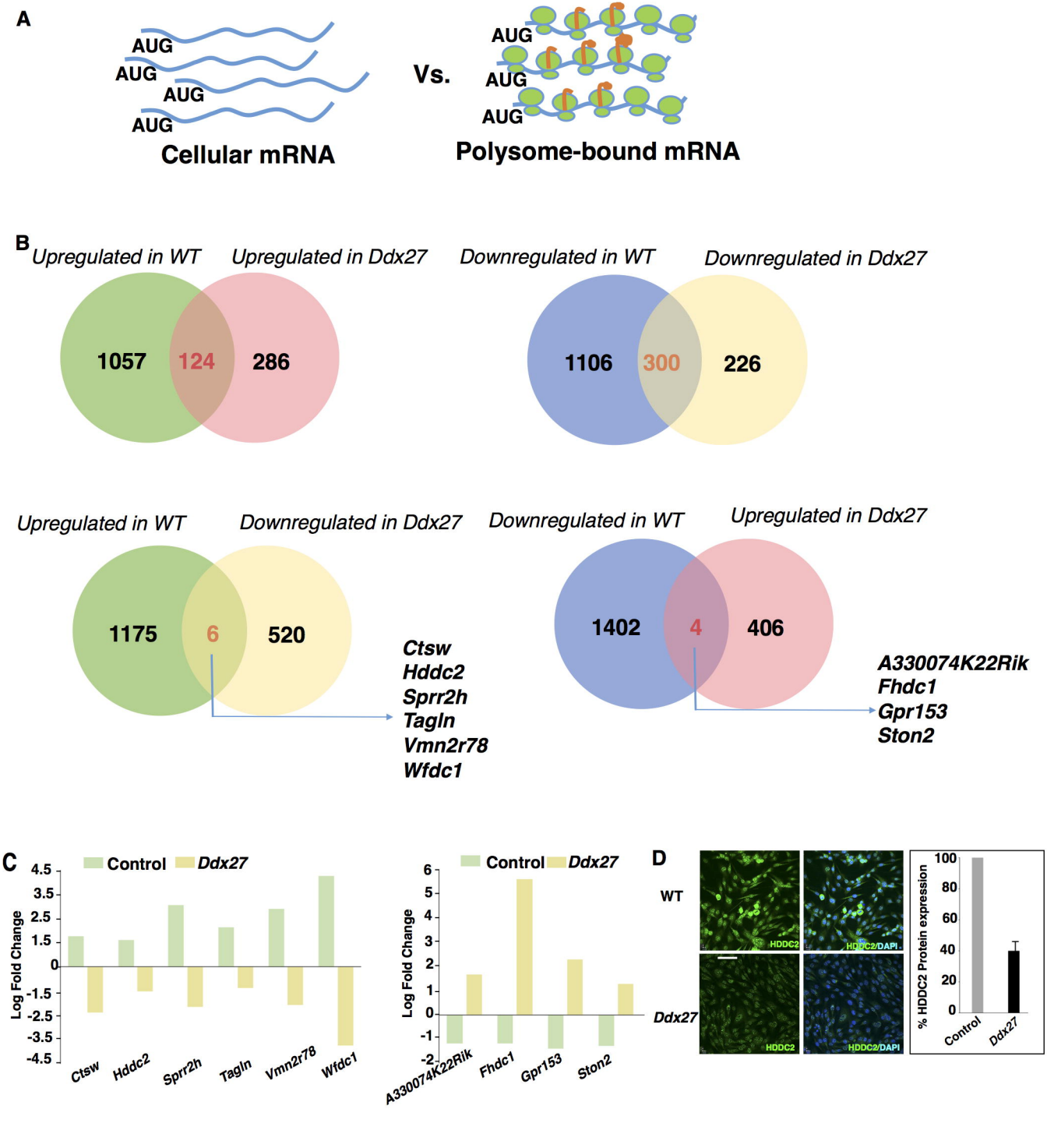
A
AUG
AUG
AUG
AUG
Cellular mRNA
Vs.
AUG
AUG
AUG
Polysome-bound mRNA
B
Upregulated in WT
Upregulated in Ddx27
1057
124
286
Downregulated in WT
Downregulated in Ddx27
1106
300
226
Upregulated in WT
Downregulated in Ddx27
1175
6
520
Ctsw
Hddc2
Sprr2h
Tagln
Vmn2r78
Wfdc1
Downregulated in WT
Upregulated in Ddx27
1402
4
406
A330074K22Rik
Fhdc1
Gpr153
Ston2
C
Control
Ddx27
Log Fold Change
4.5
3.5
2.5
1.5
0
-1.5
-2.5
-3.5
-4.5
Ctsw
Hddc2
Sprr2h
Tagln
Vmn2r78
Wfdc1
Control
Ddx27
Log Fold Change
6
5
4
3
2
1
0
-1
-2
A330074K22Rik
Fhdc1
Gpr153
Ston2
D
WT
Ddx27
HDDC2
HDDC2/DAPI
HDDC2
HDDC2/DAPI
% HDDC2 Protein expression
100
80
60
40
20
0
Control
Ddx27